Supersonic flow past cones of general cross-section

By P. M. STOCKER† AND F. E. MAUGER
Armament Research and Development Establishment, War Office, Sevenoaks, Kent

(Received 1 December 1961)

The differential equations representing the supersonic flow of a gas past a cone of any cross-section are integrated numerically, using a method similar to those used for bluff-body problems. A stream function is used as one of the independent variables and this is particularly suitable for determining the singular 'vortical layer'. The method is here applied to the cases of elliptic cones at zero yaw and circular cones at incidence. The results are compared with experiment and with other numerical solutions.

1. Introduction

In the past few years several authors—Mangler & Evans (1957), Van Dyke & Gordon (1959), Vaglio-Laurin & Ferri (1958) and Zlotnik & Newman (1957)—have obtained satisfactory numerical solutions of the problem of hypersonic flow past a bluff-nosed body. In every case the method adopted has been what may be called an inverse marching process. The direct problem is: given the body shape, to determine the pressure on the body, the flow field around it and the shape of the shock wave it produces. The inverse method of solution is based on the use of the shock wave as starting line. A shock wave shape is chosen and all quantities are then known at the shock; it is then possible to find the whole flow field and the body shape by integrating the flow equations step-by-step away from the shock. The resulting body shape is determined and compared with the required body shape. The shock shape is then modified in such a way as to produce a body shape which approximates more closely to the one that is required and the integration is repeated. This process is continued until the required degree of accuracy is obtained. Satisfactory convergence has been obtained for sufficiently smooth bodies; for instance a spherical nosed body has been obtained to a high degree of accuracy by Van Dyke & Gordon (1959). Solutions obtained by a step-by-step method of the kind used here have been ignored until recently partly because the stability and convergence of the numerical scheme was thought to be unsatisfactory and partly because the idea of obtaining the solution of an elliptic equation from data specified on an open boundary was itself suspect. However, the solutions obtained agree well with experimental results and with one another and the method appears to be satisfactory.

The object of this paper is to apply the inverse marching procedure to a different class of problems, namely, the class which arises in 'conical' or 'similarity'

† Now at Ferranti Ltd., West Gorton, Manchester 12.

solutions and which gives rise to an elliptic differential equation involving two independent variables. The case of the supersonic flow of an ideal gas past a cone of general cross-section, which may be at incidence, is an example, the flow produced by a uniformly expanding cylinder of general section is another from the field of unsteady flow, and similar examples arise elsewhere. In fact, problems of this nature will arise in many situations which lead to a hyperbolic differential equation in three independent variables. In the more familar theory of characteristics for hyperbolic problems in two variables the solution at singular points leads to an ordinary differential equation, e.g. the Taylor–Maccoll solution for flow past an unyawed cone. At the singular points of a three-variable problem the solution of a second-order elliptic equation of the type considered here is often required.

One further aspect of step-by-step solutions must be mentioned. Most authors make use of a stream function as a variable in their computations. Van Dyke uses it as variable in the bluff-body problem, and Briggs (1959) uses a similar method

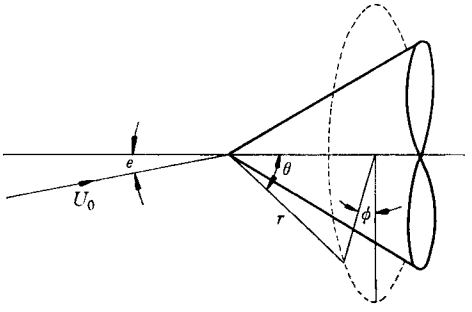

FIGURE 1. The co-ordinate system.

for the problem of flow past an elliptic cone; they determine its value in terms of space variables, which are used as independent variables. Mangler & Evans (1957) and Vaglio-Laurin & Ferri (1958) make use of the stream function in their independent variables; the flow is then determined in a non-physical plane, and the geometry of the physical plane is determined by quadrature. The latter approach will be adopted here for reasons which are given in § 2.

The specific problem treated here is that of the inviscid, steady, supersonic flow of an ideal gas past a cone of arbitrary section, but the method is applicable to a wider class of problems.

Spherical polar co-ordinates r, θ, ϕ are chosen with $r = 0$ at the cone apex, the axis $\theta = 0$ coincident with the cone axis, and the meridian plane $\phi = 0$ chosen in some convenient manner. Let p_0, ρ_0 and u_0 be, respectively, the pressure, density and velocity of the undisturbed stream. Denote by uu_0, vu_0 and wu_0 the components of fluid velocity in the directions r, θ and ϕ increasing respectively, and by $\rho_0 u_0^2 p$ and $\rho\rho_0$ the pressure and density. The co-ordinates are illustrated, for the particular case of a circular cone at incidence, in figure 1, where the plane $\phi = 0$ has been chosen as the plane of symmetry on the windward side of the body. The flows considered are 'similar' or 'conical' because of the absence of a length scale. Thus, along any ray, $\phi = \text{const.}$, $\theta = \text{const.}$, all flow quantities are inde-

pendent of r. Derivatives with respect to r vanish from the equations of flow, which are

$$v\frac{\partial u}{\partial\theta}+\frac{w}{\sin\theta}\frac{\partial u}{\partial\phi}=v^2+w^2, \tag{1.1}$$

$$v\frac{\partial v}{\partial\theta}+\frac{w}{\sin\theta}\frac{\partial v}{\partial\phi}+\frac{1}{\rho}\frac{\partial p}{\partial\theta}=w^2\cot\theta-uv, \tag{1.2}$$

$$v\frac{\partial w}{\partial\theta}+\frac{w}{\sin\theta}\frac{\partial v}{\partial\phi}+\frac{1}{\rho\sin\theta}\frac{\partial p}{\partial\phi}=-vw\cot\theta-uw, \tag{1.3}$$

$$\frac{\partial}{\partial\theta}(\rho v\sin\theta)+\frac{\partial}{\partial\phi}(\rho w)=-2u\rho\sin\theta, \tag{1.4}$$

$$v\frac{\partial S}{\partial\theta}+\frac{w}{\sin\theta}\frac{\partial S}{\partial\phi}=0, \tag{1.5}$$

$$\frac{\partial v}{\partial\theta}+\frac{1}{\sin\theta}\frac{\partial w}{\partial\phi}+\frac{v}{\rho a^2}\frac{\partial p}{\partial\theta}+\frac{w}{\rho a^2\sin\theta}\frac{\partial p}{\partial\phi}=-2u-v\cot\theta, \tag{1.6}$$

where (1.6) is a modified form of (1.4) and where S is the entropy and a the dimensionless speed of sound. The problem is to be solved in a (θ,ϕ)-plane, say $r=1$, working from the trace of the shock wave to the trace of the body surface.

2. The vortical singularity

Ferri (1951) observed that the body surface must be a surface of constant entropy and that because of this there must be a region of high vorticity near the body surface, the *vortical layer*. From equation (1.5) it is clear that entropy is conserved along a family of curves in the (θ,ϕ)-plane; these curves are the intersections of the stream surfaces of constant entropy with the unit sphere and will be referred to as 'streamlines'. The streamlines originate at the shock and for physical reasons cannot cross†; the streamlines terminate in one or more singular points in the flow at which the entropy is multivalued, the *vortical singularities*. Equation (1.5) shows that at such a point $v=w=0$. Thus these singularities represent the final direction into which the particles moving along these streamlines are deflected. The vortical singularities may be on the body or in the flow. If there are several on the body, the entropy is constant between these singularities, but may be different in different sections. In many cases the position of the vortical singularities will be determined by symmetry conditions. Thus the elliptic cone at zero incidence has a vortical singularity on the body‡ at either end of the minor axis. The circular cone at a small incidence will have one at $\phi=\pi$ on the body. With increasing incidence the singularity will move into the field. The end-points of the major axis of the elliptic cone at zero incidence and the point $\phi=0$ on the body of the circular cone at incidence behave like 'stagnation points' with $v=w=0$; $u\neq 0$.

† Except possibly at singularities with no physical significance in cases which involve additional shock waves.

‡ It seems possible that the singularity might occur off the body in extreme cases.

It is clear that in the case of a body which differs only slightly from a circular cone at zero incidence the vortical layer must be very thin and that the circular cone represents a limit which is approached non-uniformly. It will appear later that a very thin layer of high vorticity occurs in all cases.

The importance of the entropy in the vortical layer necessitates the use of a variable which varies significantly across the vortical layer, and the geometrical variables θ and ϕ are clearly not suitable for this purpose. What is needed is a stream function, but the conical equations (1.1) to (1.6) are fundamentally three-dimensional equations and hence a single stream function does not exist. It is possible, however, to introduce two stream functions (Krzywoblocki 1958). Let ψ and σ be such that

$$\sigma \frac{\partial \psi}{\partial \phi} = -\rho v \sin\theta, \tag{2.1}$$

$$\sigma \frac{\partial \psi}{\partial \theta} = \rho w. \tag{2.2}$$

Consider the use of ϕ and ψ as independent variables. Then

$$\left(\frac{\partial}{\partial \phi}\right)_\theta = \left(\frac{\partial}{\partial \phi}\right)_\psi - \frac{\rho v \sin\theta}{\sigma}\left(\frac{\partial}{\partial \psi}\right)_\phi, \tag{2.3}$$

and

$$\left(\frac{\partial}{\partial \theta}\right)_\phi = \frac{\rho w}{\sigma}\left(\frac{\partial}{\partial \psi}\right)_\phi. \tag{2.4}$$

Equation (1.5) becomes

$$\left(\frac{\partial S}{\partial \phi}\right)_\psi = 0, \tag{2.5}$$

and therefore the 'streamlines' are lines $\psi = \text{const.}$ The variable ψ is therefore a suitable choice as one of the independent variables. Moreover, if ψ is chosen as independent variable, the region of solution is automatically limited to the fluid and there is no necessity to consider the flow at 'imaginary' points inside the body, a situation which arises if geometrical co-ordinates are used.

The choice of the second independent variable must now be considered. The angular variable ϕ is not satisfactory because for the unyawed circular cone the lines $\phi = \text{const.}$ coincide with the family $\psi = \text{const.}$ Again, θ is not satisfactory because it is insensitive in the vortical layer for near-circular cones. On inspection it is found that σ (or rather a variable closely related to it) is suitable.

From equations (2.1) and (2.2) it follows that

$$\left(\frac{\partial}{\partial \theta}\right)_\phi \left(\frac{\rho v \sin\theta}{\sigma}\right) + \left(\frac{\partial}{\partial \phi}\right)_\theta \left(\frac{\rho w}{\sigma}\right) = 0,$$

which can be simplified by use of equation (1.4) to obtain

$$-\frac{1}{\sigma}\left(\frac{\partial \sigma}{\partial \phi}\right)_\psi = \frac{2u \sin\theta}{w}. \tag{2.6}$$

It is convenient to define η such that

$$\eta = \log\{F(\psi)/\sigma\}, \tag{2.7}$$

where $F(\psi)$ is a function to be chosen later. Then

$$\left(\frac{\partial \eta}{\partial \phi}\right)_{\psi} = \frac{2u \sin\theta}{w}. \tag{2.8}$$

The shock wave is chosen to be the curve $\eta = 0$ and thus $\sigma = F(\psi)$ at the shock. If the function $F(\psi)$ is chosen arbitrarily then ψ is defined at the shock wave apart from an unimportant constant. If ψ is chosen arbitrarily at the shock then $F(\psi)$ can be determined from equations (2.1) and (2.2). Also, at the vortical singularity, $v = w = 0$, whereas $(\partial\psi/\partial\phi)_\theta$ and $(\partial\psi/\partial\theta)_\phi$ are non-zero, and hence equations (2.1) and (2.2) imply that $\sigma = 0$ at the vortical singularity. Thus η is infinite there.

The numerical procedure is to start from the line $\eta = 0$ and to integrate the equations one step so as to find the solution along the line $\eta = h = \text{const.}$; another integration gives the solution on $\eta = 2h$, and so on. In this way the solution is computed along 'streamlines' which approach the vortical singularity, but do not attain it in a finite number of steps. This is desirable because the body shape is defined by the dividing 'streamline' (but see § 5), and it is convenient to be able to determine the shape of this without the complication which would arise if other 'streamlines' had reached the singularity.

3. The equations of motion

The equations of motion with ψ and η as independent variables are

$$\frac{\partial u}{\partial \eta} = \frac{v^2 + w^2}{2u}, \tag{3.1}$$

$$\frac{\partial v}{\partial \eta} - \frac{\sin\theta}{\sigma}\frac{\partial \phi}{\partial \psi}\frac{\partial p}{\partial \eta} = \frac{w^2 \cot\theta}{2u} - \frac{v}{2} - \frac{w}{2u\sigma}\frac{\partial p}{\partial \psi}, \tag{3.2}$$

$$\frac{\partial w}{\partial \eta} + \frac{v \sin\theta}{w\sigma}\frac{\partial \phi}{\partial \psi}\frac{\partial p}{\partial \eta} + \frac{1}{\rho w}\frac{\partial p}{\partial \eta} = -\frac{vw \cot\theta}{2u} - \frac{w}{2} + \frac{v}{2u\sigma}\frac{\partial p}{\partial \psi}, \tag{3.3}$$

$$\frac{1}{\rho a^2}\frac{\partial p}{\partial \eta} + \frac{1}{w}\left(1 + \frac{\rho v \sin\theta}{\sigma}\frac{\partial \phi}{\partial \psi}\right)\frac{\partial w}{\partial \eta} - \frac{\rho \sin\theta}{\sigma}\frac{\partial \phi}{\partial \psi}\frac{\partial v}{\partial \eta} = \frac{\rho v}{2u\sigma}\frac{\partial w}{\partial \psi} - \frac{\rho w}{2u\sigma}\frac{\partial v}{\partial \psi} - 1 - \frac{v \cot\theta}{2u}, \tag{3.4}$$

$$\frac{\partial \rho}{\partial \eta} = \frac{1}{a^2}\frac{\partial p}{\partial \eta}, \tag{3.5}$$

$$\frac{\partial \phi}{\partial \eta} = \frac{w}{2u \sin\theta}, \tag{3.6}$$

$$\frac{\partial \theta}{\partial \eta} = \frac{v}{2u}. \tag{3.7}$$

3.1. *Boundary conditions*

At any point on the shock surface let Ω be the angle between a normal to the surface and the plane $\phi = \text{const.}$ through the point, considered positive if the normal lies on the side of greater ϕ. Let α be the angle between the normal and the free-stream direction, and let ϵ be the angle of incidence, i.e. the angle between the line

$\theta = 0$ and the free-stream direction. Then the following relations hold immediately behind the shock:

$$u = -\sin\theta\cos\phi\sin\epsilon + \cos\theta\cos\epsilon,$$

$$v = -\rho^{-1}\cos\Omega\{(\cos\theta\cos\phi\sin\epsilon + \sin\theta\cos\epsilon)\cos\Omega - \sin\phi\sin\Omega\sin\epsilon\}$$
$$-\sin\Omega\{(\cos\theta\cos\phi\sin\epsilon + \sin\theta\cos\epsilon)\sin\Omega + \sin\phi\sin\epsilon\cos\Omega\},$$

$$w = -\rho^{-1}\sin\Omega\{(\cos\theta\cos\phi\sin\epsilon + \sin\theta\cos\epsilon)\cos\Omega - \sin\phi\sin\Omega\sin\epsilon\}$$
$$+\cos\Omega\{(\cos\theta\cos\phi\sin\epsilon + \sin\theta\cos\epsilon)\sin\Omega + \sin\phi\sin\epsilon\cos\Omega\},$$

$$p = \frac{2}{\gamma+1}\cos^2\alpha - \frac{\gamma-1}{\gamma(\gamma+1)}\frac{1}{M_0^2}, \qquad \rho = \frac{\cos^2\alpha}{\frac{\gamma-1}{\gamma+1}\cos^2\alpha + \frac{2}{\gamma+1}\frac{1}{M_0^2}},$$

where M_0 is the free-stream Mach number.

If $f(\theta, \phi) = 0$ defines the shock surface then

$$\cos\alpha = -(\cos\theta\cos\phi\sin\epsilon + \sin\theta\cos\epsilon)f_\theta[f_\theta^2 + f_\phi^2\sin^{-2}\theta]^{-\frac{1}{2}}$$
$$+\sin\phi\sin\epsilon\operatorname{cosec}\theta f_\phi[f_\theta^2 + f_\phi^2\sin^{-2}\theta]^{-\frac{1}{2}},$$

and

$$\cos\Omega = f_\theta[f_\theta^2 + f_\phi^2\sin^{-2}\theta]^{-\frac{1}{2}}.$$

4. The numerical solution

The equations of § 3, with boundary conditions as in § 3.1, were integrated by the inverse marching technique using a Ferranti Mark 1* digital computer. The shock shape was represented in all cases by a Fourier cosine series in the form

$$\sin^2\theta = a_0 + \sum_1^n a_r\cos r\phi. \tag{4.1}$$

In order to provide an equal interval difference scheme in ψ the following method is adopted. Let $\psi = \phi$ at the shock wave, then because ψ is continuous at the shock

$$F(\psi) = \sigma = -(\rho v\sin\theta + \rho w f_\phi/f_\theta), \tag{4.2}$$

which is the required boundary condition for σ at the shock. Elsewhere, from equation (2.7), it follows that

$$\sigma = F(\psi)\exp(-\eta). \tag{4.3}$$

The equations are now integrated in the following manner. All quantities which occur in equations (3.1) to (3.7) are known at the shock wave, $\eta = 0$. The ψ-derivatives of these quantities are evaluated using a nine-point difference formula, i.e.

$$(\Delta\psi)(\partial x/\partial\psi)_0 = A_1(x_1 - x_{-1}) + A_2(x_2 - x_{-2}) + A_3(x_3 - x_{-3}) + A_4(x_4 - x_{-4}),$$
$$A_1 = 0{\cdot}8, \quad A_2 = -0{\cdot}2, \quad A_3 = 0{\cdot}03809524, \quad A_4 = -0{\cdot}00357143,$$

use being made of symmetries at the end-points. The values of the η-derivatives can now be found by solving the set of simultaneous equations (3.1) to (3.7).

Values of all quantities on the line $\eta = h$ are now given by

$$x(h) = x(0) + (\partial x/\partial\eta)_0 h,$$

and σ is found from (4.3). The whole process is then repeated to advance the integration one step further, and so on.

5. Results for particular examples

It has long been thought that the step-by-step solution of elliptic equations is unsatisfactory because the solution is necessarily unstable. No analytical treatment of stability or convergence has been attempted. A degree of instability, ranging from slight to catastrophic has been observed in the various cases (§ 6). The object of the present section is to present the computed results, to discuss their physical significance, and to compare them with experimental results and with other similar work.

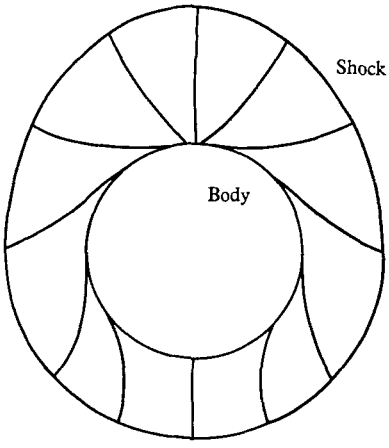

FIGURE 2. A section of a yawed circular cone showing the lines of constant entropy or 'streamlines'.

The cases computed were as follows.

A. Indirect cases in which the shock shape was prescribed and the body shape determined.

(i) A series of cases of shocks at zero incidence ($\epsilon = 0$) with infinite free-stream Mach number ($M_0 = \infty$). The Fourier series representation of the shock wave was used (equation (4.1)) and a_0 was held constant at a value of 0·166 whilst a_2 was varied. This leads to a series of shocks of oval section, with approximately constant mean angle and varying eccentricity.

(ii) Two cases of shocks of nearly elliptic section at zero incidence.

(*a*) $\epsilon = 0$, $M_0 = 10$, $\tan\theta_{\max} = 0{\cdot}5$, $\tan\theta_{\min} = 0{\cdot}4$;

(*b*) $\epsilon = 0$, $M_0 = 6$, $\tan\theta_{\max} = 0{\cdot}962$, $\tan\theta_{\min} = 0{\cdot}577$.

B. Direct cases in which the body shape was prescribed, and the shock shape determined by iteration.

(i) A body of elliptic section at zero incidence†

$$\epsilon = 0, \quad M_0 = 6, \quad \tan\theta_{\max} = 0{\cdot}400, \quad \tan\theta_{\min} = 0{\cdot}226.$$

(ii) Two cases of a circular cone at incidence.

The cone having a semi-angle of 20°, in each case $M_0 = 3{\cdot}53$, and (*a*) $\epsilon = 5°$, (*b*) $\epsilon = 10°$.

† This body is only a close approximation to an ellipse, see Ferri (1959).

The cases A (i) were the first to be computed; a typical case, $a_2 = -0{\cdot}03$, is shown in figure 3. It can be seen that, not only do the 'streamlines' converge on the vortical singularity, but they appear to touch at the body surface before they reach the singularity. That is the body appears to be an envelope of 'streamlines'; a 'streamline', after entering the vortical layer, rapidly approaches the body

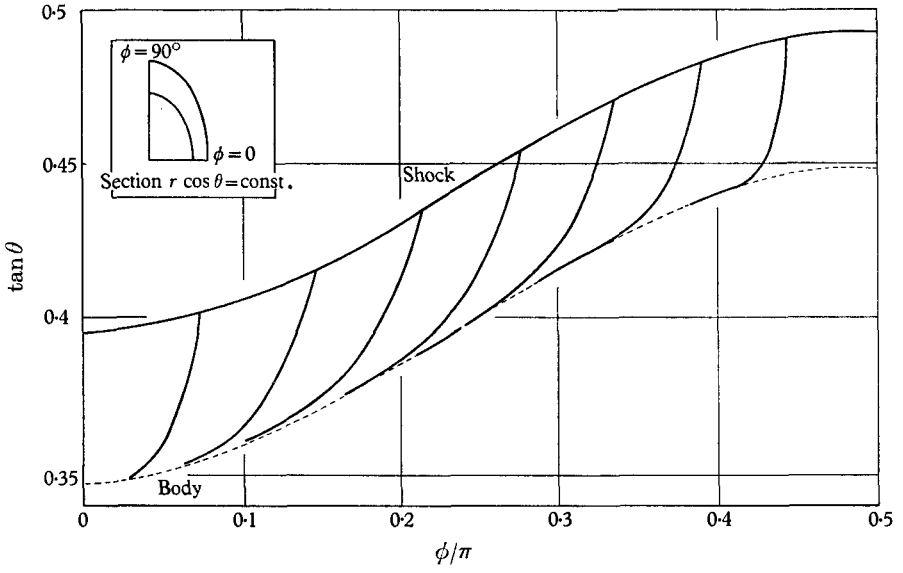

FIGURE 3. Conical shock at infinite Mach number.

surface. This behaviour was observed in all cases, not merely in those slightly different from the unyawed cone, and a mathematical analysis shows that the distance between 'streamlines' in the layer decreases exponentially with distance along the lines. Because of this 'envelope'-like behaviour it was unnecessary to determine the shape of the 'dividing streamline', the one which actually defines the body, in order to determine the body shape. Moreover, the pressure varies little across the vortical layer and 'streamline' points in the (ψ, η)-plane which correspond to the same point in the physical plane yield the same pressure. However, the quantities u, v, w and ρ vary rapidly across the layer, and the profile cannot be found from the computed solution, although they could possibly be determined by fitting a solution for the vortical layer.

The case A (i)

A typical case $a_0 = 0{\cdot}166$, $a_2 = -0{\cdot}03$ is shown in figure 3 which shows the shock and body shapes and the 'streamlines'. In this, and in other cases with a high Mach number, the graph is plotted on a rectangular grid so that the region between the shock and body may be magnified. Figure 4 shows lines of constant density. A plot of isobars was not made because, around $\phi = 45°$, they lie too closely parallel to the 'streamline' to prepare an accurate figure. The pressure around the body is shown in figure 5.

In cases where $a_2 < -0{\cdot}055$ no satisfactory body shape was obtained. For such cases the shock has become concave near $\phi = 0$. Even a slight concavity in the shock produced a violent concavity in the body near $\phi = 0$ and the solution

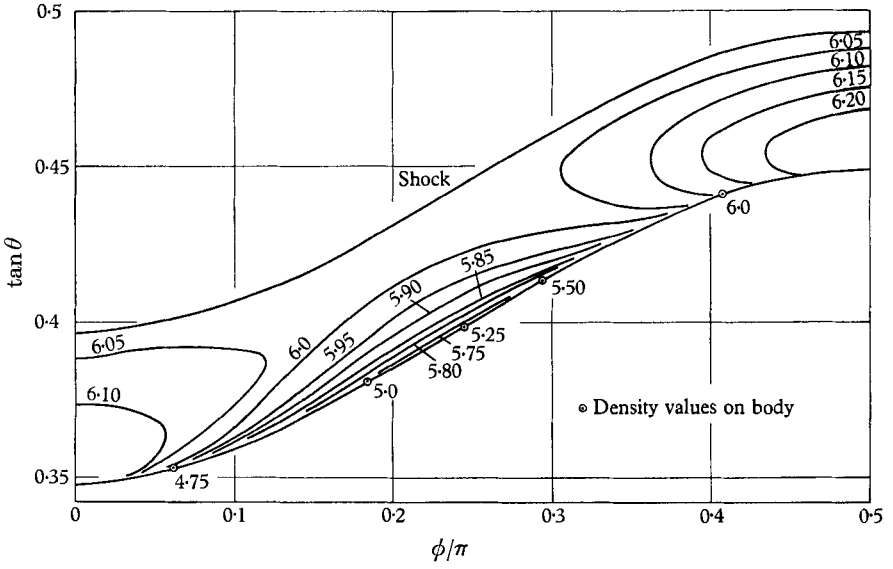

FIGURE 4. Isopycnics for a case of a conical shock at infinite Mach number.

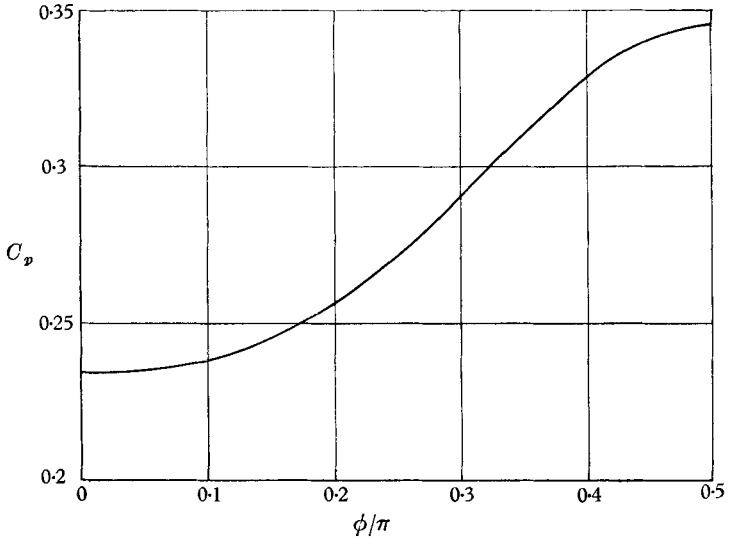

FIGURE 5. Body pressures for a case of an elliptic conical shock at infinite Mach number.

became so inaccurate that it was impossible to say whether such shocks yielded a concave body or whether, in fact, they could not be produced by any body.

A case $a_0 = 0{\cdot}155$, $a_2 = -0{\cdot}06$, $a_4 = 0{\cdot}011$ was computed. This has the same axes as a case $a_0 = 0{\cdot}166$, $a_2 = -0{\cdot}06$, but a different shape. It is not concave near $\phi = 0$ and produced a satisfactory body shape. Thus it becomes clear that small changes in shock shape can produce appreciable differences in body shape.

The cases A (ii)

These cases were carried out in order to compare the present theory with two other numerical techniques. Mauger (1960) has computed the solution to problem A (ii) (*a*) by using a method similar to that which Garabedian (1957) used for the bluff-body problem. This method is known to be stable, but is extremely long, and the time taken would be excessive if a direct problem were to be solved. The method is based on the use of characteristics in a complex plane and in the form

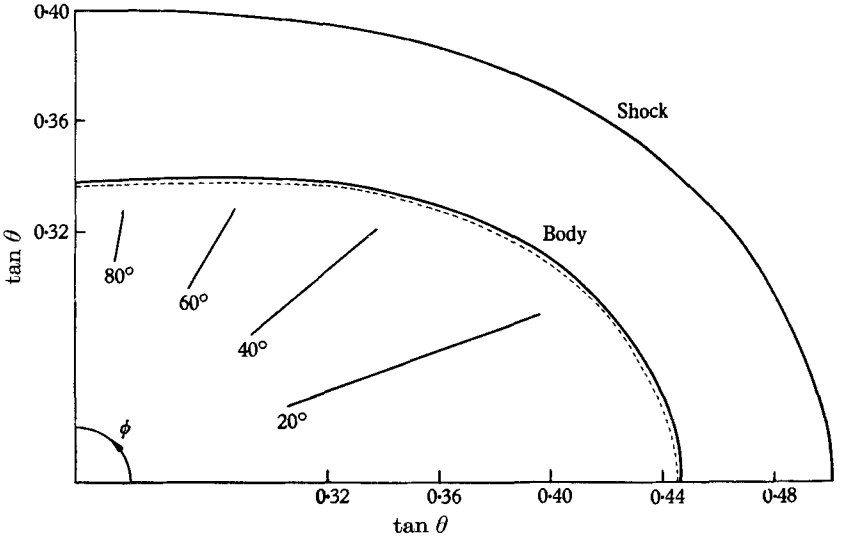

FIGURE 6. Comparison of two methods for a conical shock of elliptic cross-section at Mach number 10. – – –, Body derived by Mauger.

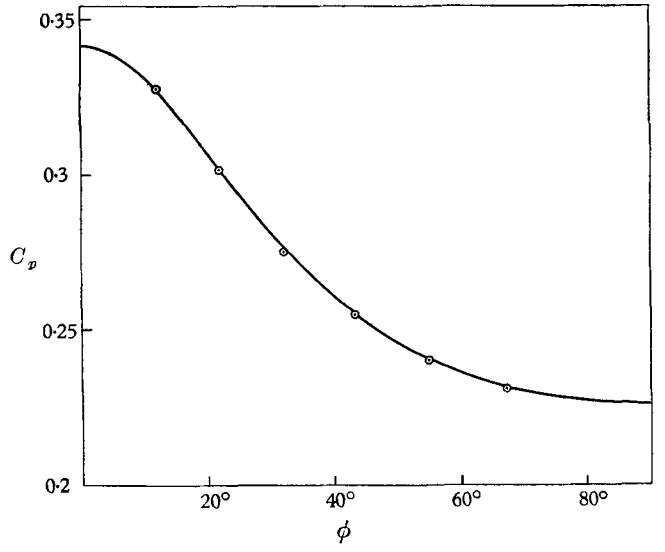

FIGURE 7. Pressure coefficient on the body given by an elliptic conical shock at $M = 10$. ——, Present method; ⊙, Mauger's method.

used by Mauger difficulty is experienced near the body, because the lines on which the solution is computed cross the vortical layer, whereas in the method described here they lie in it. Satisfactory agreement between the two methods has been

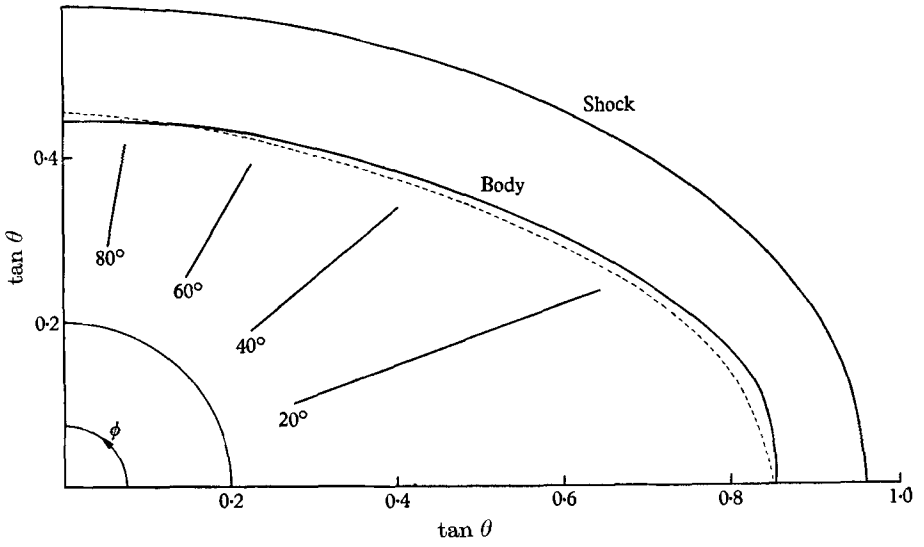

FIGURE 8. Comparison of two methods for a conical shock of elliptic cross-section ($M = 6$). – – –, Body derived by Briggs.

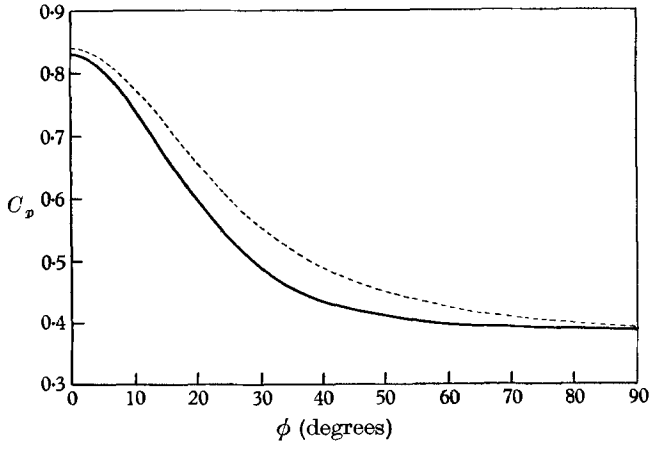

FIGURE 9. Body pressures for the case of a conical shock of elliptic cross-section ($M = 6$). – – –, Pressures derived by Briggs; —, pressures derived by present method.

obtained. The resulting body shapes are shown in figure 6, and the body pressure distributions in figure 7. For better comparison of the two methods figure 6 has been drawn with a false origin.

Case A (ii) (*b*) was computed for comparison with the results of Briggs (1959) who also used a marching technique, but who computes the solution using physical space variables as independent variables. In its present form his method uses an

elliptic co-ordinate system and only elliptic shocks can be considered. A comparison of the bodies resulting from the two methods is shown in figure 8, and the pressures are compared in figure 9.

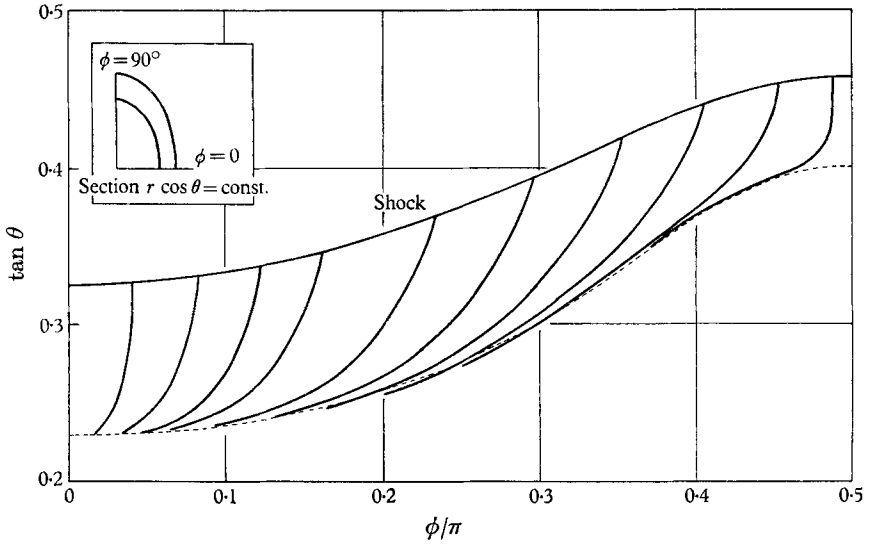

FIGURE 10. The flow over a conical body of elliptic cross-section ($M = 6$).

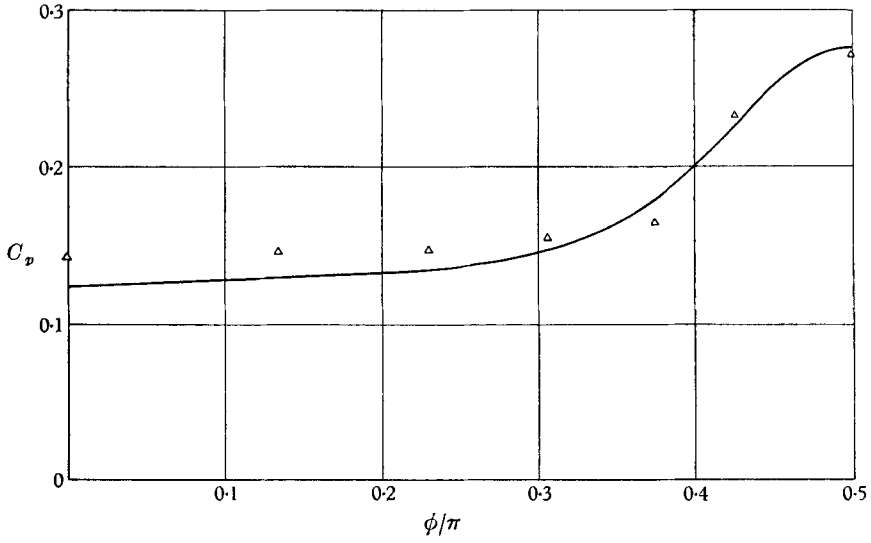

FIGURE 11. Body pressures for the case of a conical body with elliptic cross-section ($M = 6$). △, Experimental pressures (Ferri).

The case B (i)

This was a direct problem in that the shock shape corresponding to a given body shape was found. The body chosen was one of approximately elliptic section which had been studied experimentally by Ferri (1959). Initially a shock shape was guessed and a solution computed using large steps to save time. The shock was

then modified empirically to obtain a closer approximation to the required shape and when close agreement was reached a smaller step size was used. In all, five cases were computed, the values of the shock wave coefficients being tabulated

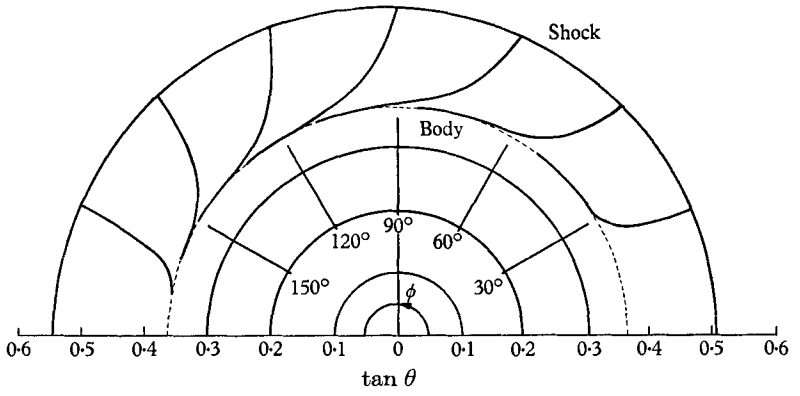

FIGURE 12. Flow over a yawed circular cone. Semi-apex angle of cone = 20°. Mach number = 3·53. Angle of yaw = 5°.

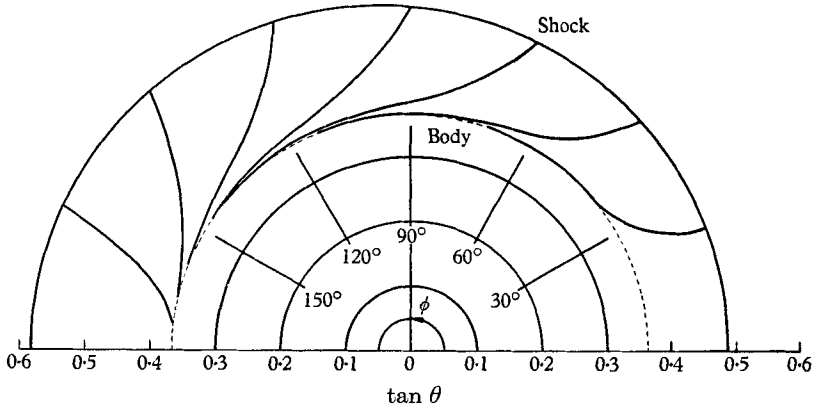

FIGURE 13. Flow over a yawed circular cone. Semi-apex angle of cone = 20°. Mach number = 3·53. Angle of yaw = 10°.

Case	a_0	a_2	a_4	a_6
1	0·125	−0·050	0·006	0
2	0·125	−0·042	0·006	0
3	0·127	−0·037	0·006	−0·003
4	0·129	−0·039	0·006	−0·001
5	0·1284	−0·0379	0·006	−0·0007

TABLE 1

in table 1. The 'streamlines' are shown together with the required 'envelope' in figure 10; the comparison between the experimental and theoretical pressure distributions is shown in figure 11. The agreement is satisfactory, particularly if allowance is made for a boundary layer near the vortical singularity.

The cases B (ii)

The figures 12 and 13 show the shock shapes and 'streamline' shapes for a cone of 20° semi-angle at $M = 3{\cdot}53$ for the cases of 5° and 10° incidence respectively. The isobars for 10° incidence are shown in figure 14 and the isopycnics in figure 15. Figure 16 shows the pressure distribution on the body and experimental points

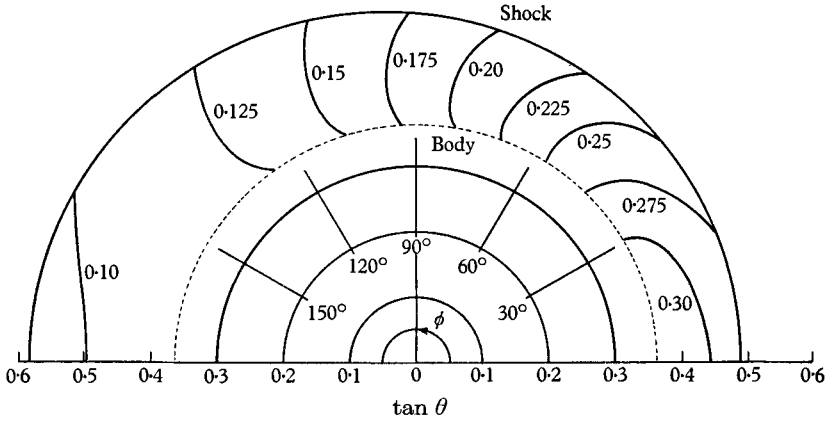

FIGURE 14. Isobars for a yawed circular cone (intervals in the pressure coefficient C_p). Semi-apex angle of cone = 20°. Mach number = 3·53. Angle of yaw = 10°.

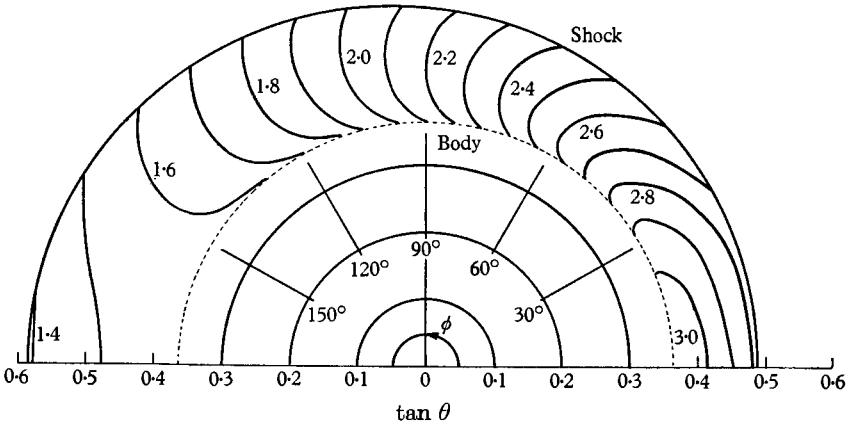

FIGURE 15. Isopycnics for a yawed circular cone (intervals of ρ/ρ_0). Semi-apex angle of cone = 20°. Mach number = 3·53. Angle of yaw = 10°.

from Holt & Blackie (1956) are included for comparison. The agreement is good on the windward but not so satisfactory on the leeward side near the vortical singularity.

The computation of the 10° case brought to light a property of the computed solution which became much more marked as the incidence increased and which made it impossible to obtain a satisfactory solution for cases of higher incidence. In the initial solution of these problems a Fourier series terminating at a_5 was used. In the 10° case it was found that, after suitably choosing the coefficients, this led

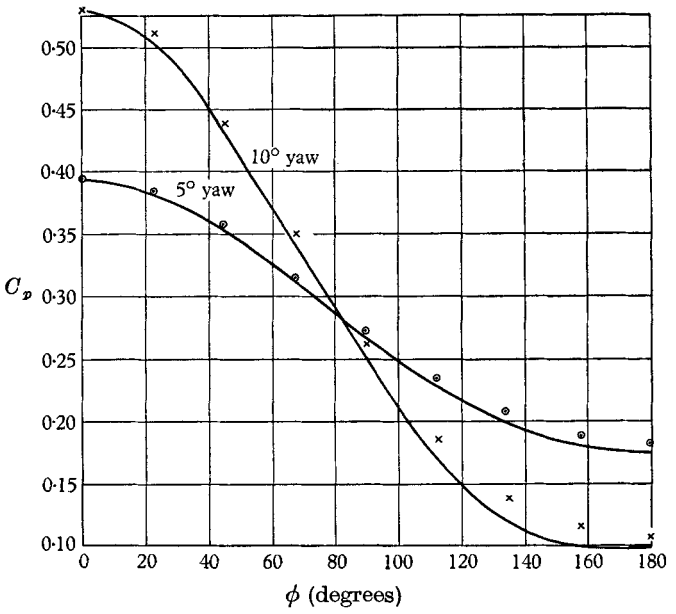

FIGURE 16. Body pressures on yawed circular cones. Semi-apex angle = 20°, M = 3·53. ⊙, ×, Experimental pressures (Holt & Blackie).

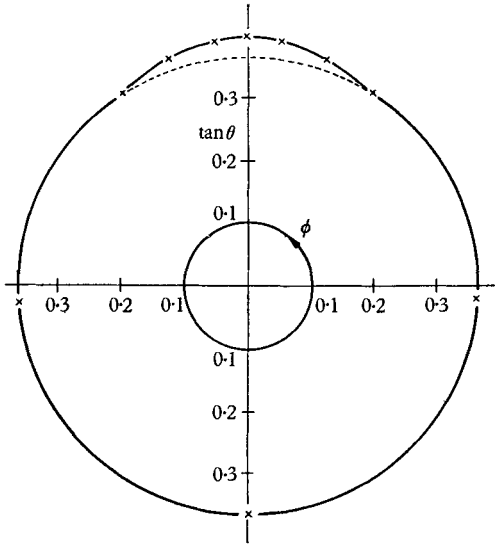

FIGURE 17. A case of a yawed circular cone illustrating the leeward bump and the last computed points. Semi-apex angle of cone = 20°. Mach number = 3·53. Angle of yaw = 15°.

to a body which was very nearly circular for the range $\phi = 0$ to $\phi = 150°$, but which then produced a small hump on the circular cone in the range $\phi = 150°$ to $\phi = 210°$ (figure 17). In order to eliminate this hump it was necessary to introduce a corresponding 'hollow' in the shock near $\phi = 180°$, though not so severe as to make a concave shock. It was found that this had to be done in an analytic way, and for this purpose the coefficients in the Fourier series for the shock profile were

generated by using the finite Fourier series for $\sin^n \phi/2$, where the index n was chosen to match the hollow required. With a little effort satisfactory results were obtained for the 10°-incidence case, but the 15°-incidence case did not respond to this treatment and a circular body could not be obtained near the vortical singularity. A likely explanation for this failure of the method is this: the shock belongs to a cone at a higher incidence where the vortical singularity lies outside the body on $\phi = \pi$; the accuracy of the method (which in this area uses a technique of marching along the body) is not sufficient to establish a 'stagnation' point on the body at $\phi = \pi$ (which would close it) and then to continue towards the vortical singularity outside the body.

6. Concluding remarks

The accuracy of the solution in any particular case is believed to be demonstrated in two ways:

(*a*) by the accuracy of the 'envelope' formed by the streamlines;

(*b*) by the accuracy of the values for the pressure in the layer, i.e. points which are widely separated in the (ψ, η)-plane but which yield nearly coincident points in the layer should have almost identical pressures.

In cases where the Mach number was large and the ellipticity small the accuracy in this sense was very high. As the Mach number decreases, or as the body becomes more elliptic or the incidence higher the accuracy decreased. This is clearly to be expected; for low supersonic Mach numbers the shock shape varies little from a circle and small changes at the shock will produce large changes at the body. The computation of anything other than extremely simple body shapes is unlikely to be possible. A computation was carried out for the case considered by Radhakrishnan (1958). This is the case of a circular *shock* with a stream at incidence. The resulting streamlines were very wild and no well-defined body shape resulted. It is likely that in practice a rather complicated body shape would be needed to produce this shock. Cases with a concave shock also led to streamline patterns which did not converge.

It is not very difficult to explain why the numerical solution is unsatisfactory near the vortical singularity. The equations of motion may be thought of as having a solution which falls into three régimes. First, there is the majority of the field between shock and body; in this region the solution may be thought of as 'non-singular' and computation is straightforward. When the vortical layer is entered the solution is still regular from the mathematical point of view but 'singular' as regards its numerical behaviour; terms which are formerly dominant in the equations now balance each other identically, so that terms which formerly were less dominant now start to govern motion. From the computational point of view great care must be taken to formulate the problems in the correct way and terms must be grouped so as to obtain the maximum possible accuracy. As the vortical singularity is approached the present numerical method becomes more and more inadequate to cope with the associated mathematical singularity and the asymptotic behaviour as the singularity is approached is probably incorrect. This is not likely to have much effect on the pressure which tends to be remarkably

uniform around the vortical singularity; temperature and density (in the absence of diffusion effects) vary from streamline to streamline.

The difficulty with the case at incidence is interesting. The vortical singularity will detach from the body with increasing incidence and the point $\phi = \pi$ on the body will change in character and turn into a 'stagnation' point. The streamline pattern will not be very complicated but in a large region the (v, w)-components of the velocity will be too small for the present method to work satisfactorily.

Finally it should be noted that the details of the behaviour of the vortical layer are important for all three-dimensional problems of this type and must be clarified before full use can be made of three-dimensional characteristic methods such as that of Butler (1960).

The authors wish to thank Miss P. L. Wright for the very considerable help she gave in carrying out these computations.

REFERENCES

Briggs, B. P. 1959 Calculation of supersonic flow past bodies shaped like elliptic cones. *NASA Rep.* no. D-24.

Butler, D. S. 1960 The numerical solution of hyperbolic systems of partial differential equations in three independent variables. *Proc. Roy. Soc.* A, **255**, 232.

Ferri, A. 1951 Supersonic flow around circular cones at angles of attack. *NACA Rep.* no. 1045.

Ferri, A. 1959 Review of recent developments in hypersonic flow. *Adv. Aero. Sci.* **2**, 744. (London: Pergammon Press.)

Garabedian, P. R. 1957 Numerical construction of detached shock waves. *J. Math. Phys.* **36**, 192.

Holt, M. & Blackie, J. 1956 Experiments on circular cones at yaw in supersonic flow. *J. Aero. Sci.* **23**, 931.

Krzywoblocki, M. Z. v. 1958 On the stream functions in non-steady three dimensional flow. *J. Aero. Sci.* **25**, 67.

Mangler, K. W. & Evans, N. E. 1957 Unpublished Ministry of Supply Report.

Mauger, F. E. 1960 Unpublished War Office Report.

Radhakrishnan, R. 1958 The exact flow behind a yawed conical shock. *College of Aeronautics, Cranfield, Rep.* no. 116.

Vaglio-Laurin, R. & Ferri, A. 1958 Theoretical investigation of the flow field about blunt-nosed bodies in supersonic flight. *J. Aero. Sci.* **25**, 761.

Van Dyke, M. D. & Gordon, H. D. 1959 Supersonic flow past a family of blunt axisymmetric bodies. *NASA Rep.* no. R-1.

Zlotnik, M. & Newman, D. J. 1957 Theoretical calculation of the flow on blunt-nosed bodies in a hypersonic stream. *AVCO RAD*-TR-2-57-29.